

Article

On the Reconstruction Peculiarities of Sol–Gel Derived $Mg_{2-x}M_x/Al_1$ ($M = Ca, Sr, Ba$) Layered Double Hydroxides

Ligita Valeikiene ¹, Marina Roshchina ², Inga Grigoraviciute-Puroniene ¹, Vladimir Prozorovich ², Aleksej Zarkov ¹, Andrei Ivanets ² and Aivaras Kareiva ^{1,*}

¹ Institute of Chemistry, Faculty of Chemistry and Geosciences, Vilnius University, Naugarduko 24, LT-03225 Vilnius, Lithuania; ligita.valeikiene@chgf.vu.lt (L.V.); inga.grigoraviciute@gmail.com (I.G.-P.); aleksej.zarkov@chf.vu.lt (A.Z.)

² Institute of General and Inorganic Chemistry of National Academy of Sciences of Belarus, st. Surganova 9/1, 220072 Minsk, Belarus; che.roschina@bsu.by (M.R.); vladimirprozorovich@gmail.com (V.P.); andreiivanets@yandex.by (A.I.)

* Correspondence: aivaras.kareiva@chgf.vu.lt; Tel.: +37061567428

Received: 6 May 2020; Accepted: 30 May 2020; Published: 2 June 2020



Abstract: In this study, the reconstruction peculiarities of sol–gel derived $Mg_{2-x}M_x/Al_1$ ($M = Ca, Sr, Ba$) layered double hydroxides were investigated. The mixed metal oxides (MMO) were synthesized by two different routes. Firstly, the MMO were obtained directly by heating $Mg(M)-Al-O$ precursor gels at 650 °C, 800 °C, and 950 °C. These MMO were reconstructed to the $Mg_{2-x}M_x/Al_1$ ($M = Ca, Sr, Ba$) layered double hydroxides (LDHs) in water at 50 °C for 6 h (pH 10). Secondly, in this study, the MMO were also obtained by heating reconstructed LDHs at the same temperatures. The synthesized materials were characterized using X-ray powder diffraction (XRD) analysis and scanning electron microscopy (SEM). Nitrogen adsorption by the Brunauer, Emmett, and Teller (BET) and Barrett, Joyner, and Halenda (BJH) methods were used to determine the surface area and pore diameter of differently synthesized alkaline earth metal substituted MMO compounds. It was demonstrated for the first time that the microstructure of reconstructed MMO from sol–gel derived LDHs showed a “memory effect”.

Keywords: layered double hydroxides; sol–gel processing; alkaline earth metals; mixed metal oxides; reconstruction effect; surface properties

1. Introduction

Layered double hydroxides ($[M^{2+}_{1-x}M^{3+}_x(OH)_2]^{x+}(A^{y-})_{x/y} \cdot zH_2O$, where M^{2+} and M^{3+} are divalent and trivalent metal cations, respectively, and A^{y-} is a intercalated anion, LDHs) are widely used in catalysis, in ion-exchange processes, as catalyst support precursors, adsorbents, anticorrosion inhibitors, anion exchangers, flame retardants, polymer stabilizers, and in pharmaceutical applications, optics, in separation science and photochemistry [1–7]. The most common preparation technique of LDHs is the co-precipitation method starting from the soluble salts of the metals [8–10]. The second synthetic technique also widely used for the preparation of LDHs is anion exchange [11–13]. Recently, for the preparation of Mg_3Al_1 LDHs, we developed the indirect sol–gel synthesis route [14–17]. In this synthetic approach, the synthesized $Mg-Al-O$ precursor gels were converted to the mixed metal oxides (MMO) by heating the gels at 650 °C. The LDHs were fabricated by the reconstruction of MMO in deionized water at 80 °C. The proposed sol–gel synthesis route for LDHs showed some benefits over the co-precipitation and anion-exchange methods such as simplicity, high homogeneity, and good

crystallinity of the end synthesis products, effectiveness, cost efficiency, and suitability for the synthesis of different LDH compositions.

Recently, this newly developed sol–gel synthesis method has been successfully applied for the synthesis of the transition metal substituted layered double $Mg_{3-x}M_x/Al_1$ ($M = Mn, Co, Ni, Cu, Zn$) [18]. Calcined at temperatures higher than 600–650 °C, the M/Mg/Al LDHs form $M_xMg_{1-x}Al_2O_4$ solid solutions having the spinel structure and various cations distributions [19–23]. It was reported that these spinel structure compounds obtained at high temperatures cannot be reconstructed to the LDHs [24–29].

The investigation of mixed oxides derived from calcined LDHs prepared by direct and indirect methods is an interesting topic, since the reformation conditions could have an effect not only on the composition of a solid but also on the morphology of oxides and consequently on the properties. Usually, the calcined LDHs materials or mixed metal oxides have high surface areas. During the calcination, the dehydroxylation of LDHs with different chemical composition gave rise to the crystal deformation and interstratified structure of metal oxides, resulting in the development of mesopores and enhancement of specific surface area and enhanced sorption capacity [30–34]. Interestingly, the obtained MMO sometimes can preserve the morphology of the LDH precursor and show also the efficient recycling of the spent adsorbent [35,36]. It has been found that the nature of the partially introduced cation into the M^{2+} position influences the conditions of thermal decomposition of LDHs and also the structural and morphological features of the formed mixed metal oxides [37]. The obtained data can be used to synthesize the oxide supports with desired adsorption and other physical properties. In this study, the alkaline earth metal substituted $Mg_{2-x}M_x/Al_1$ ($M = Ca, Sr, Ba$) layered double hydroxides were synthesized by an indirect sol–gel method. The aim of this study was to decompose the sol–gel-derived LDHs at different temperatures and investigate the possible reconstruction of obtain mixed metal oxides to LDHs. The surface area and porosity as important characteristics of these alkaline earth metal substituted MMO materials were investigated in this study as well.

2. Experimental

Aluminium nitrate nonahydrate ($Al(NO_3)_3 \cdot 9H_2O$, 98.5%, Chempur, Plymouth, MI, USA), magnesium nitrate hexahydrate ($Mg(NO_3)_2 \cdot 6H_2O$, 99.0% Chempur, Plymouth, MI, USA), calcium nitrate tetrahydrate ($Ca(NO_3)_2 \cdot 4H_2O$, 99%, Chempur, Plymouth, MI, USA), strontium nitrate ($Sr(NO_3)_2$, 99.0%, Chempur, Plymouth, MI, USA) and barium nitrate ($Ba(NO_3)_2$, 99.0%, Chempur, Plymouth, MI, USA) were used as metal sources in the preparation of $Mg_{2-x}M_x/Al_1$ ($M = Ca, Sr, Ba$) layered double hydroxides. In the sol–gel processing, citric acid monohydrate ($C_6H_8O_7 \cdot H_2O$, 99.5%, Chempur, Plymouth, MI, USA) and 1,2-ethanediol ($C_2H_6O_2$, 99.8%, Chempur, Plymouth, MI, USA) were used as complexing agents. Ammonia solution (NH_3 , 25%, Chempur, Plymouth, MI, USA) was used to change pH of the solution.

For the synthesis of $Mg_{2-x}M_x/Al_1$ ($M = Ca, Sr, Ba$; x is a molar part of substituent metal) LDHs, the stoichiometric amounts of starting materials were dissolved in distilled water under continuous stirring. Citric acid was added to the above solution, and the obtained mixture was stirred for an additional 1 h at 80 °C. Then, 2 mL of 1,2-ethanediol was added to the resulting solution. The transparent gels were obtained by the complete evaporation of the solvent under continuous stirring at 150 °C. The synthesized precursor gels were dried at 105 °C for 24 h. The mixed metal oxides (MMO) were obtained by heating the gels at 650 °C, 800 °C, and 950 °C for 4 h. The $Mg_{2-x}M_x/Al_1$ ($M = Ca, Sr, Ba$) LDHs were obtained by reconstruction of the MMO in water at 50 °C for 6 h under stirring and by changing the pH of the solution to 10 with ammonia.

X-ray diffraction (XRD) analysis was performed using a MiniFlex II diffractometer (Rigaku, The Woodlands, TX, USA) ($Cu K\alpha$ radiation) in the 2θ range from 10° to 70° (step of 0.02°) with the exposition time of 2 min per step. The morphological features of MMO samples were estimated using a scanning electron microscope (SEM) Hitachi SU-70, Tokyo, Japan. Nitrogen adsorption by the Brunauer, Emmett, and Teller (BET) and Barret method was used to determine the surface area

and pore diameter of the materials (Tristar II, Norcross, GA, USA). The pore-size distribution was evaluated by the Barrett–Joyner–Halenda (BJH) procedure. Prior to analysis, the calcined samples were outgassed at 523 K for 5 h.

3. Results and Discussion

To study the reconstruction peculiarities of sol–gel derived $Mg_{2-x}M_x/Al_1$ ($M = Ca, Sr, Ba$) layered double hydroxides (LDHs), the precursor gels were firstly annealed at 650 °C, 800 °C, and 950 °C for 4 h. The XRD patterns of mixed metal oxides (MMO) obtained by heating the Mg_2/Al_1 LDHs precursor gels at different temperatures are presented in Figure 1. The XRD pattern of the sample heated at 650 °C had two XRD peaks, which show the formation of a mixed metal oxide (MMO) phase with an MgO-like structure (JCPDS No. 96-100-0054) [14]. Thermal treatment of the precursor gels at 800 °C resulted in the formation of two phases, namely MMO and a low-crystallinity spinel phase with the composition of $MgAl_2O_4$ (JCPDS No. 96-154-0776). After heating at 950 °C, evidently, the highly crystalline $MgAl_2O_4$ phase has formed along with the MgO phase.

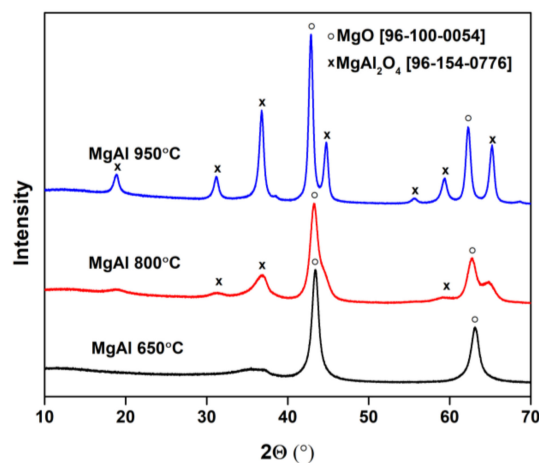


Figure 1. XRD patterns of mixed metal oxides (MMO) obtained by heating the Mg_2/Al_1 precursor gels at 650 °C, 800 °C, and 950 °C.

The XRD patterns of the Mg/Al LDH synthesized by the indirect sol–gel method (reconstruction of sol–gel derived MMO) show the formation of layered double hydroxides independent of the annealing temperature of the precursor gels (see Figure 2).

Three basal reflections typical of an LDH structure were observed: at 2θ of about 10° (003), 23° (006), and 35° (009) [14,15]. Besides, the spinel phase obtained at 800 °C and 950 °C remain almost unchanged during the reconstruction process. These results are in good agreement with those previously published elsewhere [38].

The XRD patterns of synthesis products with the same substitutional level of Ca, Sr, and Ba obtained at 800 °C and 950 °C are almost identical and revealed in all cases with the formation of crystalline magnesium oxide, magnesium spinel phase $MgAl_2O_4$ and an appropriate spinel of alkaline earth metal ($CaAl_2O_4$, $SrAl_2O_4$ and $BaAl_2O_4$). Again, during the partial reconstruction process, the phase purity of sol–gel derived $Mg_{2-x}M_x/Al_1$ LDHs evidently is dependent on the nature of introduced metal. As was expected, the spinel phases obtained at 800 °C and 950 °C remained almost unchanged during the partial reconstruction process. Moreover, during the reconstruction process, a negligible amount of metal carbonates ($CaCO_3$, $SrCO_3$, and $BaCO_3$) have formed as well. The XRD patterns of mixed metal oxides (MMO) obtained by heating the $Mg_{2-x}M_x/Al_1$ ($M = Ca, Sr, Ba$) precursor gels at different temperatures and reconstructed LDHs are presented in Figures 3–5, respectively. The XRD analysis results confirmed that the phase purity of alkaline earth substituted

LDHs obtained by an indirect sol–gel synthesis approach is highly dependent on both the annealing temperature of the precursor gels and that of the alkaline earth metal.

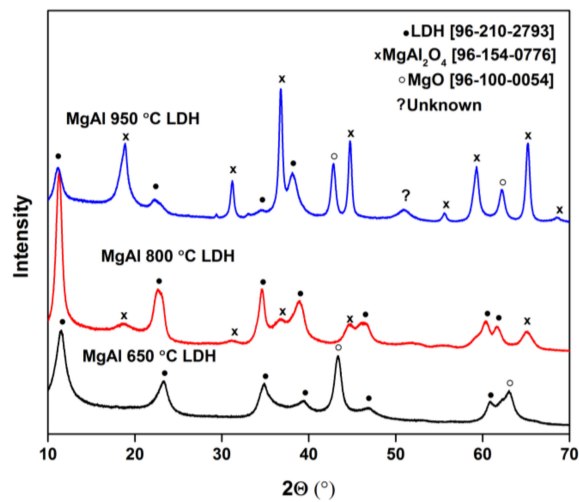


Figure 2. XRD patterns of sol–gel derived Mg_2/Al_1 layered double hydroxides (LDHs, reconstructed from MMO). The annealing temperature of the precursor gels was 650 °C, 800 °C, and 950 °C.

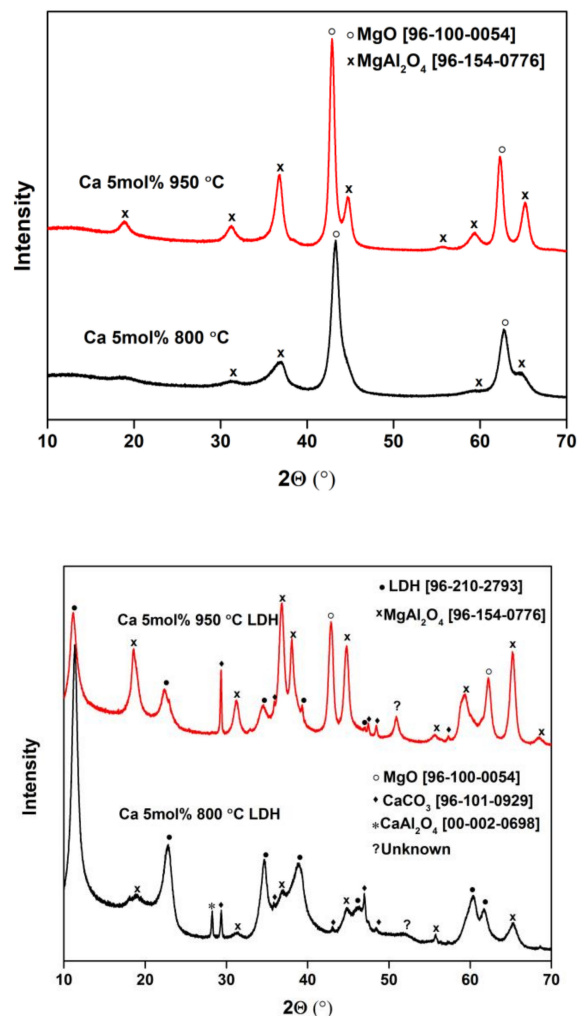


Figure 3. XRD patterns of mixed metal oxides (MMO) obtained by heating the $Mg_{1.95}Ca_{0.05}/Al_1$ precursor gels at 800 °C and 950 °C (**top**) and reconstructed $Mg_{1.95}Ca_{0.05}/Al_1$ LDHs (**bottom**).

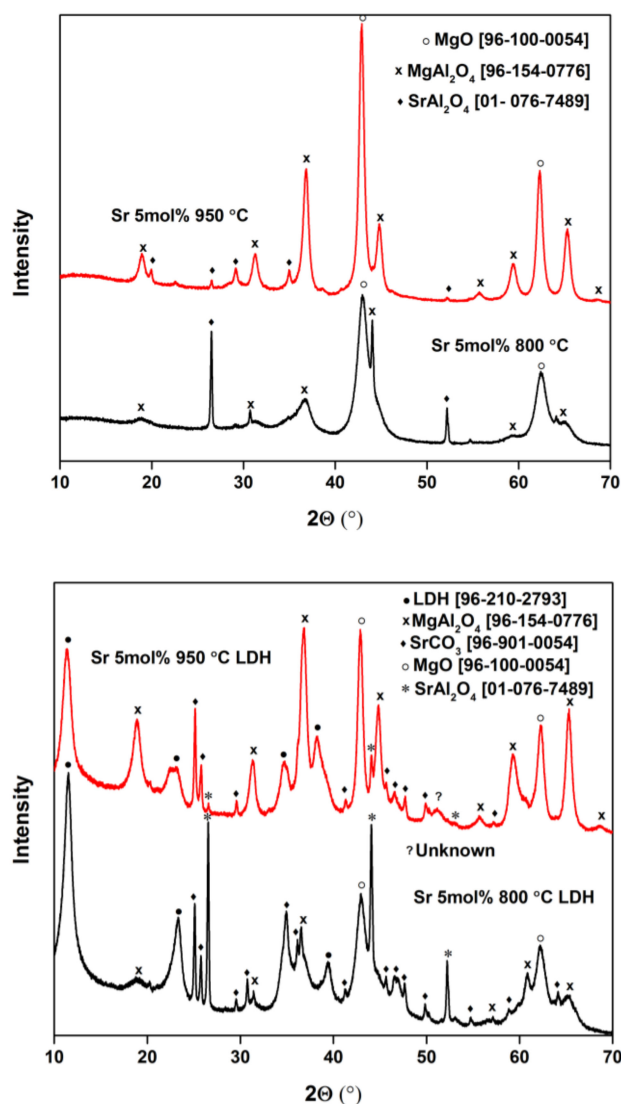


Figure 4. XRD patterns of mixed metal oxides (MMO) obtained by heating the Mg_{1.95}Sr_{0.05}/Al₁ precursor gels at 800 °C and 950 °C (**top**) and reconstructed Mg_{1.95}Sr_{0.05}/Al₁ LDHs (**bottom**).

The obtained mixed metal LDH samples were repeatedly heated at different temperatures to obtain MMO and compare the phase composition, morphology, and surface properties with obtained ones after initial annealing. The XRD patterns of non-substituted and Ca, Sr, and Ba containing MMO obtained after the heating of LDHs are shown in Figures 6 and 7, respectively. Evidently, the XRD patterns of mixed metal oxides (MMO) obtained by heating the Mg₂/Al₁ precursor gels (see Figure 1) and obtained by heating the Mg₂/Al₁ LDHs (Figure 6) are very similar, confirming the same phase composition. However, the reflections of just obtained MMO are more intense in comparison with ones presented in the repeatedly obtained MMO from LDHs. Obviously, the second time obtained Ca and Sr substituted MMO samples contain much more side phases (see Figures 3, 4 and 7). However, this is not the case for the Ba-substituted MMO samples. Both synthesis products obtained from precursor gels and by heating LDHs were composed of several crystalline phases.

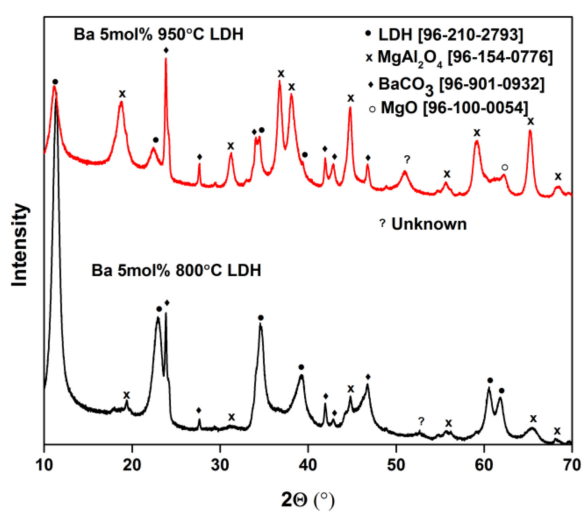
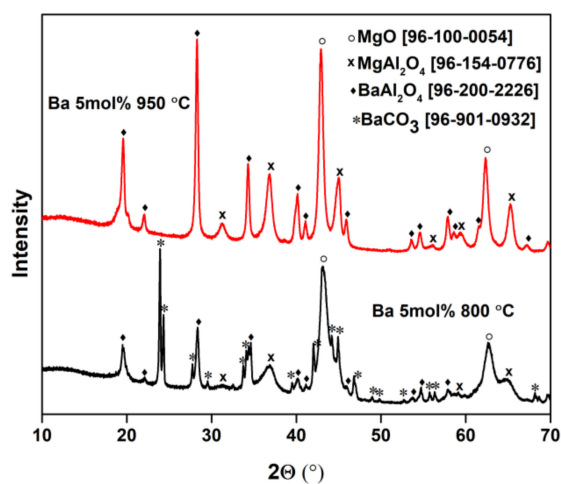


Figure 5. XRD patterns of mixed metal oxides (MMO) obtained by heating the Mg_{1.95}Ba_{0.05}/Al₁ precursor gels at 800 °C and 950 °C (**top**) and reconstructed Mg_{1.95}Ba_{0.05}/Al₁ LDHs (**bottom**).

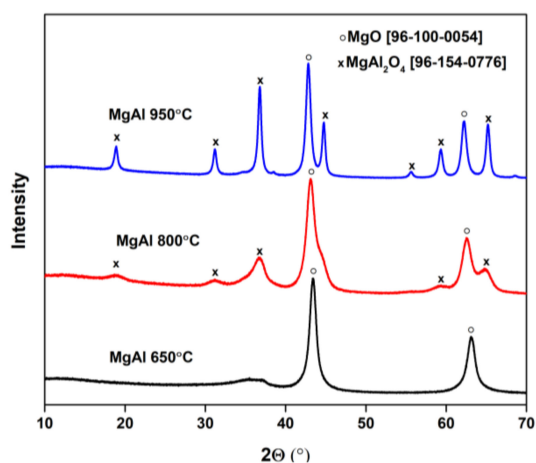


Figure 6. XRD patterns of mixed metal oxides (MMO) obtained by heating the Mg₂/Al₁ LDHs at different temperatures.

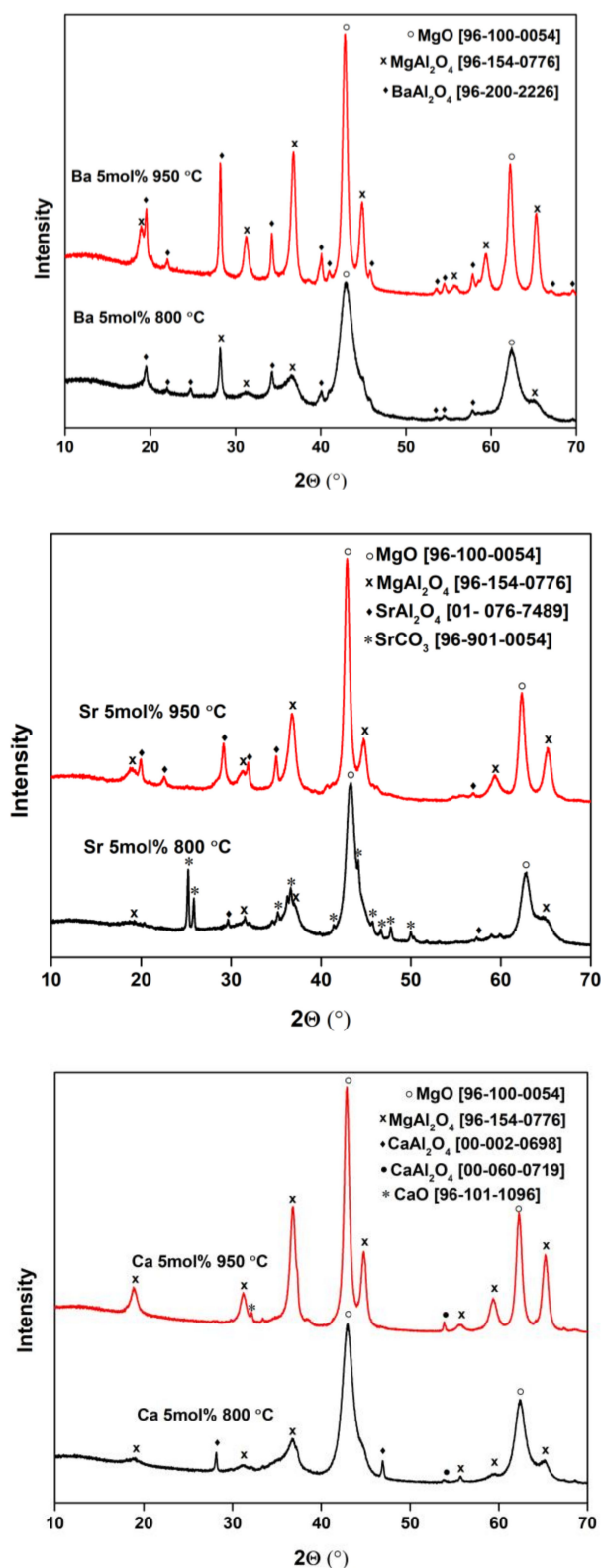


Figure 7. XRD patterns of mixed metal oxides (MMO) obtained by heating the Mg_{1.95}Ca_{0.05}/Al₁ LDHs (**bottom**), Mg_{1.95}Sr_{0.05}/Al₁ LDHs (**middle**), and Mg_{1.95}Ba_{0.05}/Al₁ LDHs (**top**) at different temperatures.

The interplanar spacings and lattice parameters of sol–gel derived Mg_{2-x}M_x/Al₁ (M = Ca, Sr and Ba) LDHs with standard deviations in parentheses are presented in Table 1.

Table 1. The interplanar spacings and lattice parameters of sol–gel derived $Mg_{1.95}M_{0.05}/Al_1$ ($M = Ca, Sr$ and Ba) LDHs.

Compound	d(003), Å	d(006), Å	d(110), Å	c, Å	a, Å
Mg_2Al_1	7.601(5)	3.810(3)	1.511(3)	22.818(3)	3.040(2)
$Mg_{1.95}Ca_{0.05}/Al_1$	7.690(4)	3.813(4)	1.512(2)	23.027(4)	3.041(3)
$Mg_{1.95}Sr_{0.05}/Al_1$	7.697(3)	3.826(3)	1.517(3)	23.034(5)	3.039(4)
$Mg_{1.95}Ba_{0.05}/Al_1$	7.695(6)	3.828(4)	1.521(1)	23.176(5)	3.041(4)

Surprisingly, the calculated values of parameter a are not increasing monotonically with the increasing ionic radius of metal in $Mg_{1.95}M_{0.05}/Al_1$. On the other hand, the amount of substituent is rather small, and the obtained LDHs were not fully monophasic.

Figures 8–11 show the morphological features of non-substituted and alkaline earth metal-substituted LDHs and MMO obtained by heating the precursor gels or Mg_2/Al_1 LDHs. The SEM micrographs of Mg–Al MMO obtained by heating Mg–Al–O precursor gel (Figure 8) confirm that the surface of synthesized compounds is composed of large monolithic particles at about 15–20 μm in size independent of the annealing temperature (800 °C and 950 °C). The surface of these monoliths is randomly covered with smaller needle-like particles, and some pores also could be detected. The SEM micrographs of reconstructed from MMO Mg_2/Al_1 LDH samples showed different morphological features. The formation of round particles (3–15 μm) could be observed, and these particles are composed of nanosized plate-like crystallites. The most interesting observation is that the surface morphology of MMO samples obtained by heating Mg_2/Al_1 LDH specimens show “memory effect”. In this case, the surface morphology of MMO is almost identical to the morphology of primary Mg_2/Al_1 LDHs. On the other hand, the morphological features of differently obtained MMO (MMO obtained by heating Mg–Al–O precursor gel and MMO obtained by heating Mg_2/Al_1 LDHs) differ considerably (see Figure 8).

The SEM micrographs of MMO obtained by heating the $Mg_{1.95}Ca_{0.05}/Al_1$ precursor gels, sol–gel derived $Mg_{1.95}Ca_{0.05}/Al_1$ LDHs, and MMO obtained by heating the $Mg_{1.95}Ca_{0.05}/Al_1$ LDHs are presented in Figure 9. The surface of Ca containing MMO obtained by heating the $Mg_{1.95}Ca_{0.05}/Al_1$ precursor gels is composed of large monolithic particles ($\geq 20 \mu m$). Apparently, the different morphological features could be determined for the reconstructed $Mg_{2-x}Ca_x/Al_1$ LDH samples. The plate-like crystals with sizes of 5–15 μm composed of nanosized plate-like crystallites have formed. An almost identical microstructure was observed for the MMO specimens obtained after heating $Mg_{2-x}Ca_x/Al_1$ LDH samples. SEM micrographs of strontium containing MMO and related $Mg_{2-x}Sr_x/Al_1$ LDHs are presented in Figure 10. The surface microstructure of Sr-containing MMO obtained by heating the $Mg_{1.95}Sr_{0.05}/Al_1$ precursor gels is very similar to the Ca-containing ones. However, on the surface of plate-like crystals of reconstructed $Mg_{2-x}Sr_x/Al_1$ LDH samples, additionally spherical particles (approximately 1 μm) were determined. These spherical particles as a “memory effect” remain on the surface of already heat-treated Sr containing LDHs. Again, the microstructure of investigated samples was not dependent on the annealing temperature. Interestingly, the barium containing $Mg_{2-x}Ba_x/Al_1$ LDH samples showed the formation of smaller LDH particles (2–5 μm) (Figure 11). The formation of plate-like crystals of MMO with the size of 7.5–12.5 μm was observed by heating these LDHs at elevated temperatures.

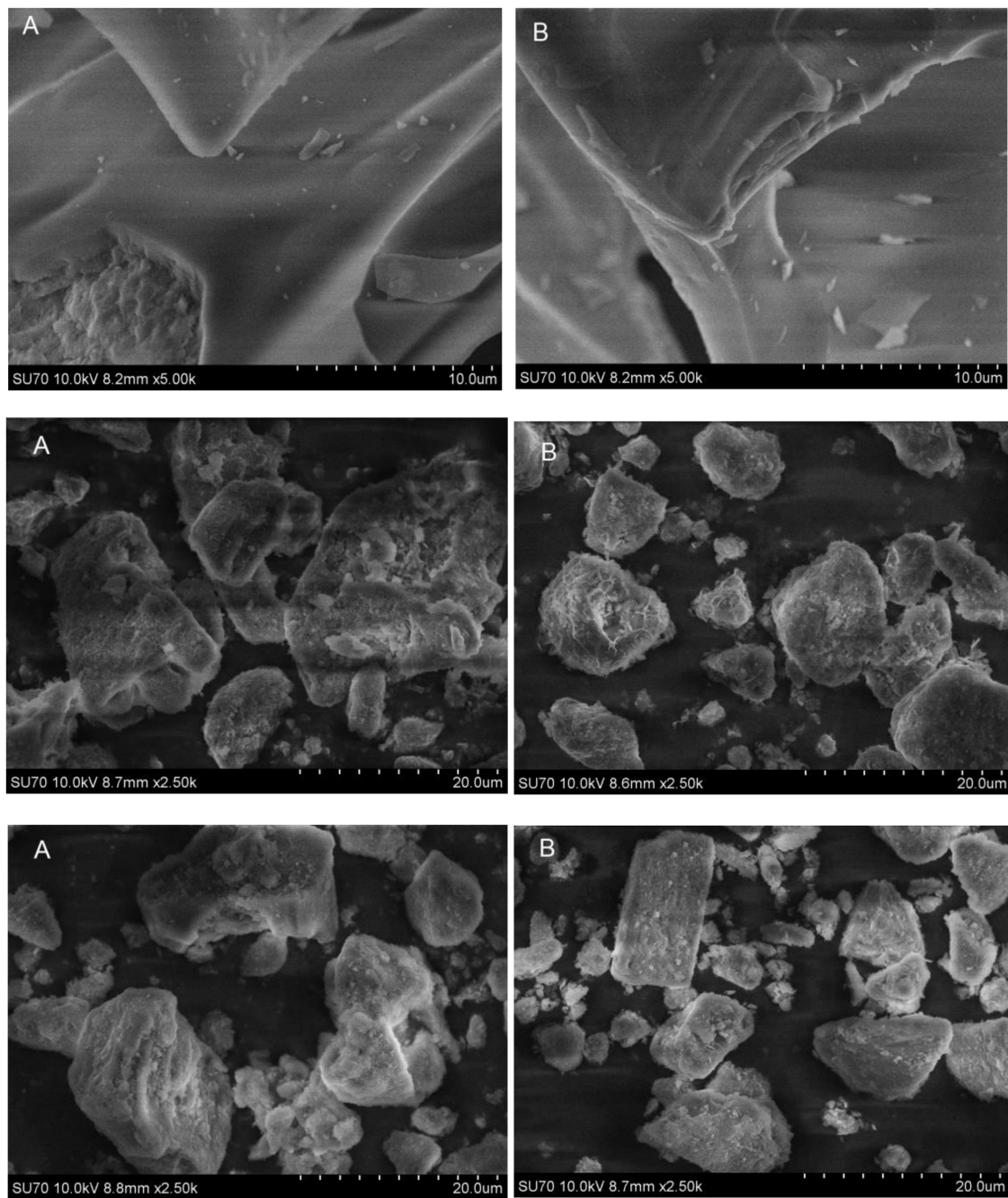


Figure 8. SEM micrographs of MMO obtained by heating the Mg_2/Al_1 precursor gels (**top**), sol-gel derived Mg_2/Al_1 LDHs (**middle**) and MMO obtained by heating the Mg_2/Al_1 LDHs (**bottom**). Annealing temperatures: 800 °C (**A**) and 950 °C (**B**).

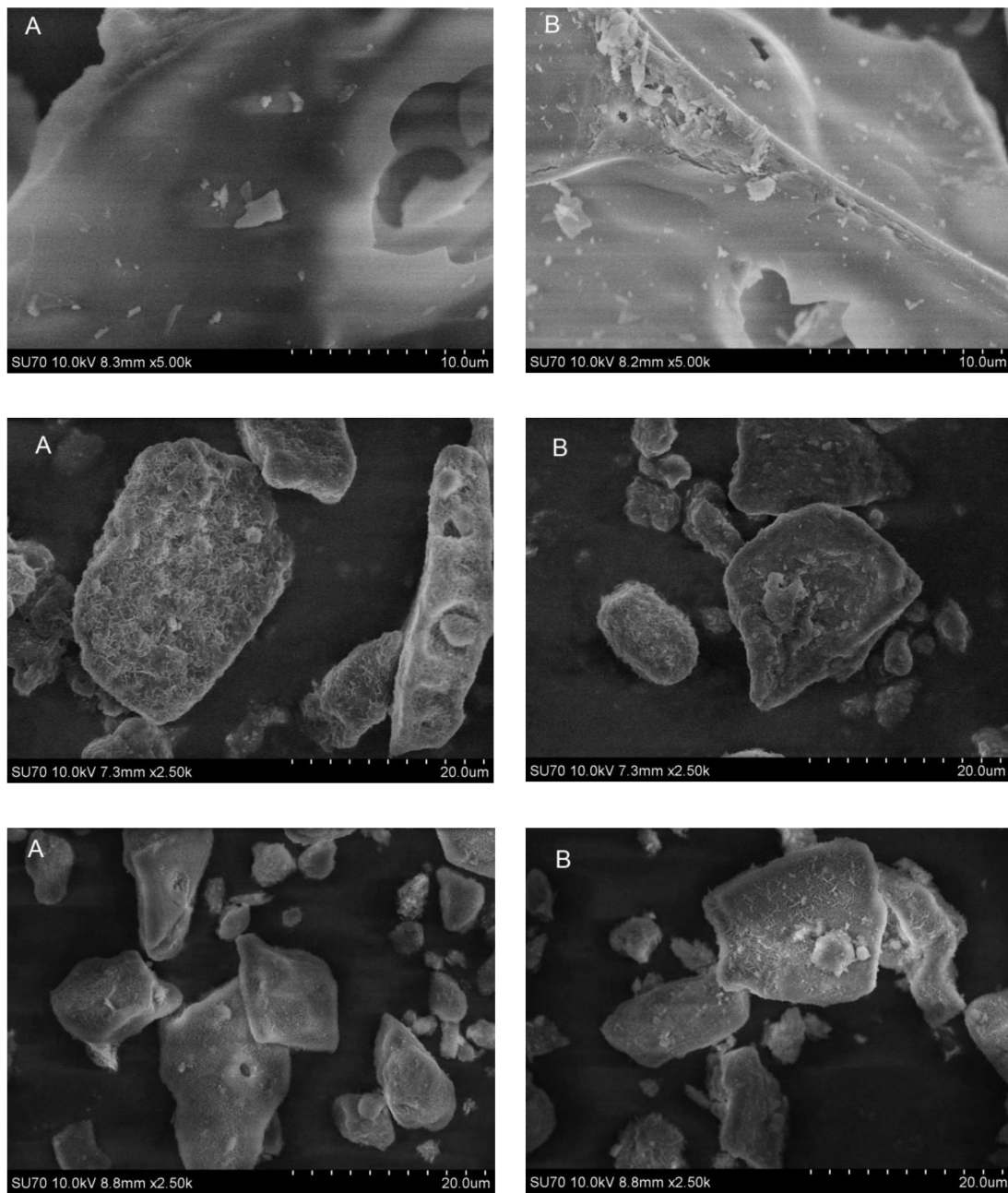


Figure 9. SEM micrographs of MMO obtained by heating the $Mg_{1.95}Ca_{0.05}/Al_1$ precursor gels (**top**), sol-gel derived $Mg_{1.95}Ca_{0.05}/Al_1$ LDHs (**middle**) and MMO obtained by heating the $Mg_{1.95}Ca_{0.05}/Al_1$ LDHs (**bottom**). Annealing temperatures: 800 °C (**A**) and 950 °C (**B**).

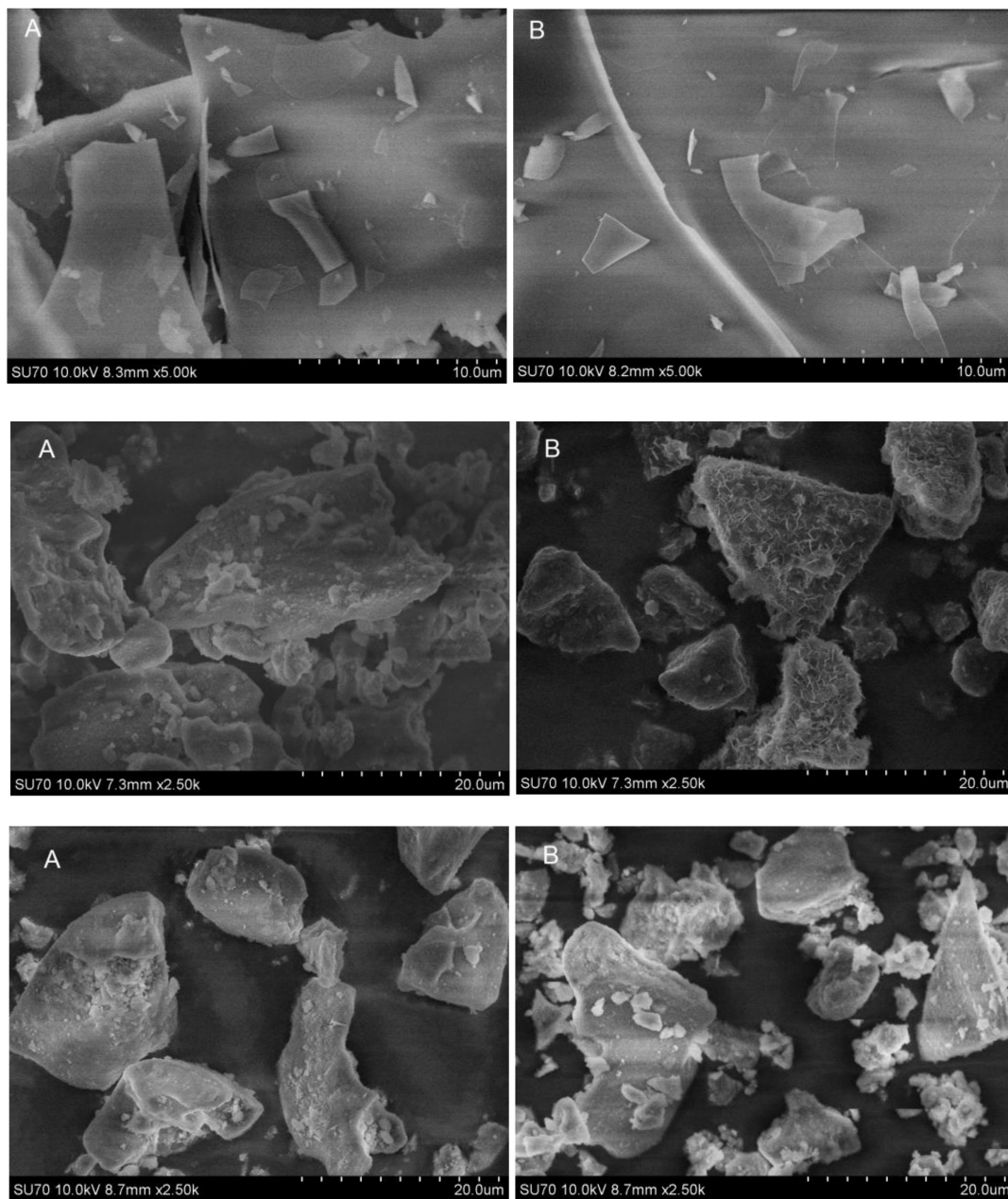


Figure 10. SEM micrographs of MMO obtained by heating the $Mg_{1.95}Sr_{0.05}/Al_1$ precursor gels (**top**), sol-gel derived $Mg_{1.95}Sr_{0.05}/Al_1$ LDHs (**middle**), and MMO obtained by heating the $Mg_{1.95}Sr_{0.05}/Al_1$ LDHs (**bottom**). Annealing temperatures: 800 °C (**A**) and 950 °C (**B**).

The results received by the BET method on Mg–Al MMO obtained by heating Mg–Al–O precursor gel and Mg_2/Al_1 LDHs are presented in Figure 12. Interestingly, these results of MMO obtained from Mg_2/Al_1 LDHs are comparable with those determined for the Mg_3/Al_1 LDH samples [18]. These samples exhibit type IV isotherms independent of the annealing temperature. At higher pressure values, the H1 hystereses are seen. This type of hysteresis is characteristic for the mesoporous (pore size in the range of 2–50 nm) materials. However, in the case of the MMO obtained by heating Mg–Al–O precursor gel, the steep increase at relatively low pressures let us predict the type of H4 isotherms, especially for the MMO samples obtained at lower temperature (800 °C). The surface area of these MMO samples evidently depends on the synthesis temperature.

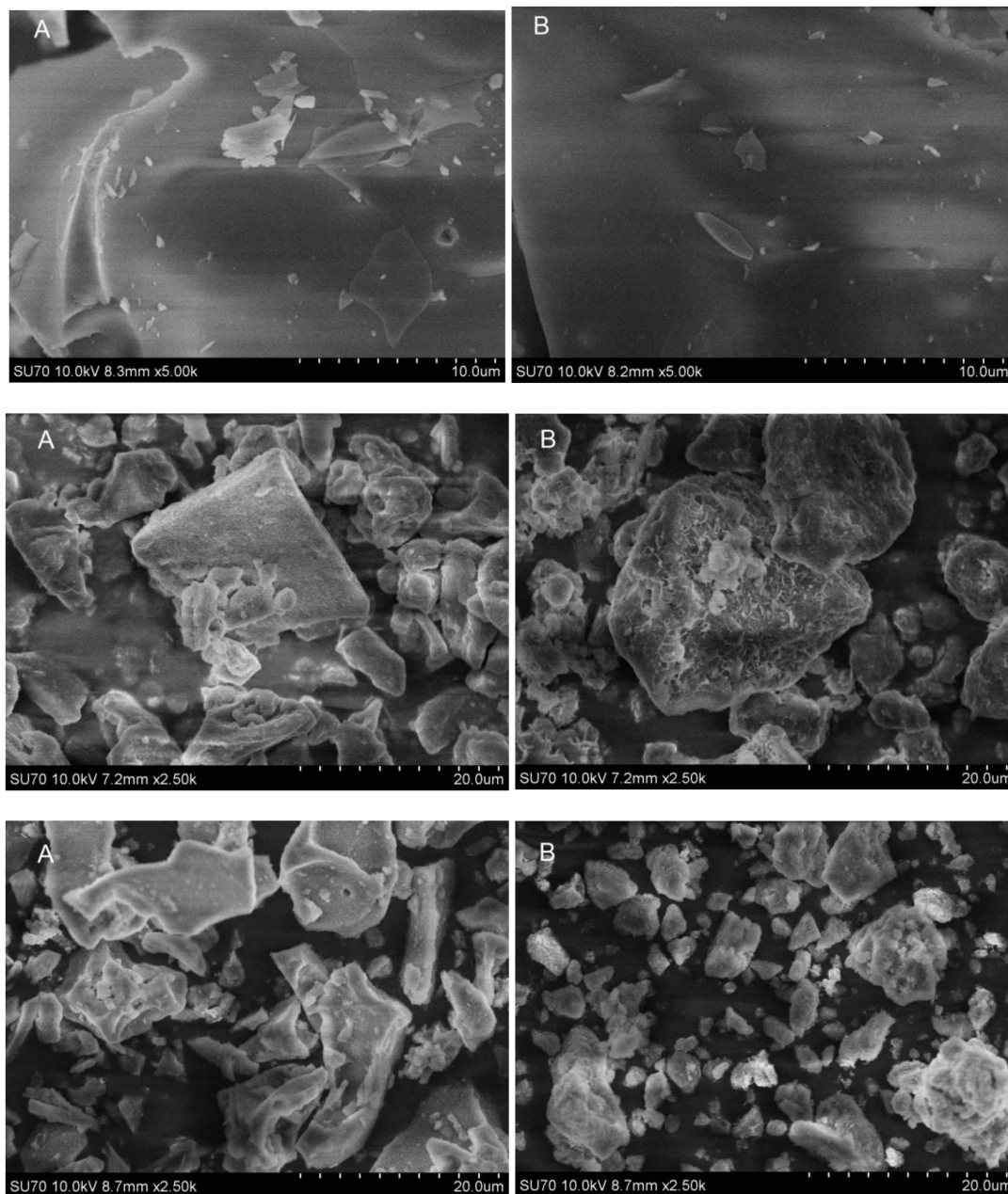


Figure 11. SEM micrographs of MMO obtained by heating the $Mg_{1.95}Ba_{0.05}/Al_1$ precursor gels (**top**), sol-gel derived $Mg_{1.95}Ba_{0.05}/Al_1$ LDHs (**middle**) and MMO obtained by heating the $Mg_{1.95}Ba_{0.05}/Al_1$ LDHs (**bottom**). Annealing temperatures: 800 °C (**A**) and 950 °C (**B**).

Thus, the isotherms and hystereses are dependent on both synthesis pathway and annealing temperature. The nitrogen adsorption–desorption results obtained for the mixed metal oxides containing Ca, Sr, and Ba (Figure 13) demonstrated that the N_2 adsorption–desorption isotherms show very similar trends.

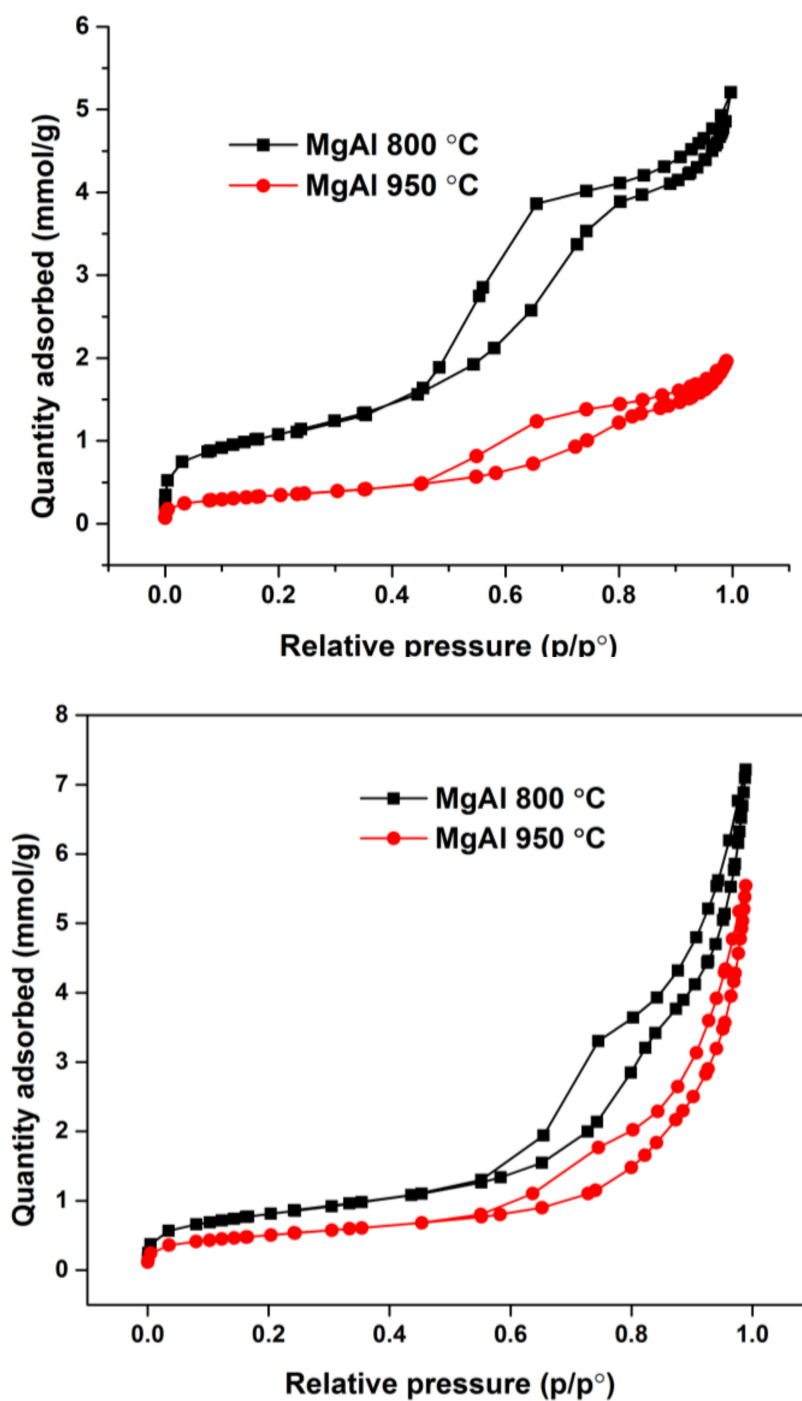


Figure 12. Nitrogen adsorption–desorption isotherms of mixed metal oxides (MMO) obtained by heating the Mg_2/Al_1 precursor gels (**top**) and obtained by heating the Mg_2Al_1 LDHs (**bottom**) at 800 °C and 950 °C.

However, in the case of barium-substituted MMO samples synthesized at 800 °C, the determined N_2 adsorption–desorption isotherms exhibited same type of isotherms independent of the synthesis method.

The results of the BET analysis of MMO samples are summarized in Table 2.

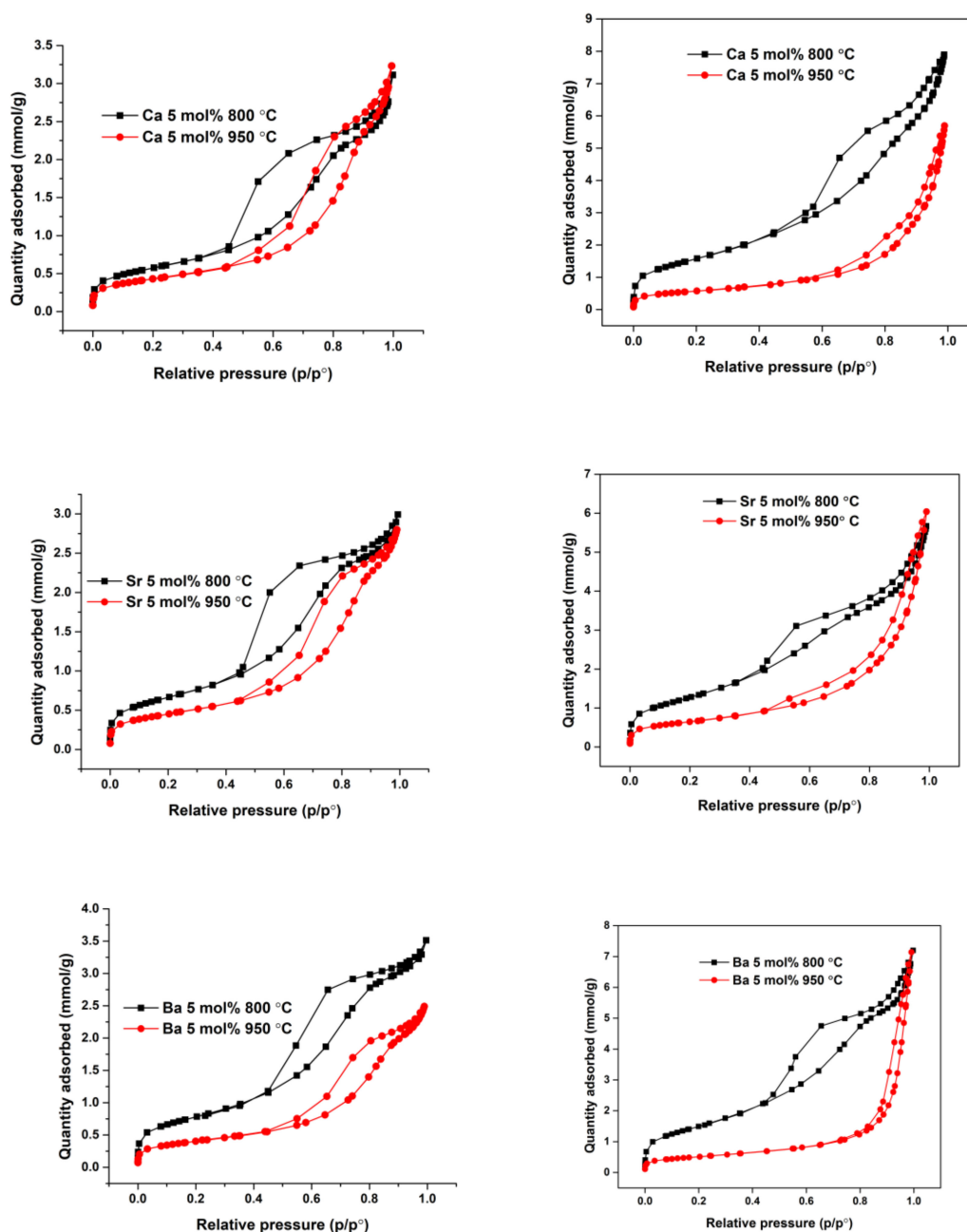
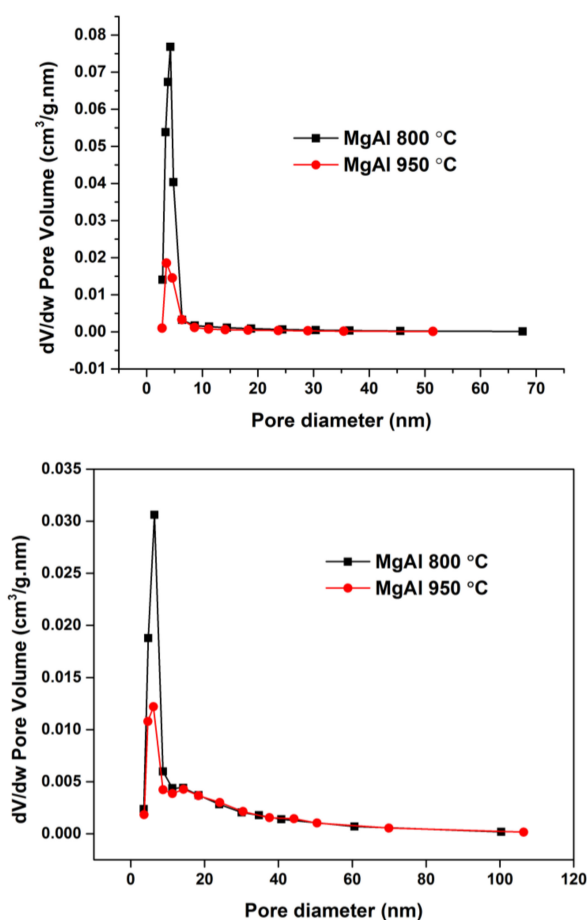


Figure 13. Nitrogen adsorption–desorption isotherms of mixed metal oxides (MMO) obtained by heating the $Mg_{1.95}Ca_{0.05}/Al_1$ precursor gels (**top, left**), by heating the $Mg_{1.95}Ca_{0.05}/Al_1$ LDHs (**top, right**), by heating the $Mg_{1.95}Sr_{0.05}/Al_1$ precursor gels (**middle, left**), by heating the $Mg_{1.95}Sr_{0.05}/Al_1$ LDHs (**middle, right**), by heating the $Mg_{1.95}Ba_{0.05}/Al_1$ precursor gels (**bottom, left**), and by heating the $Mg_{1.95}Ba_{0.05}/Al_1$ LDHs (**bottom, right**) at 800 °C and 950 °C.

Figure 14 shows the pore size distributions obtained by the BJH method for the MMO specimens obtained by heating Mg–Al–O precursor gels and Mg_2/Al_1 LDHs. Both samples demonstrate narrow pore size distributions (PSD) almost at the mesoporous level, but very close to micropores domain.

Table 2. Brunauer, Emmett and Teller (BET) surface area of sol–gel derived $Mg_{1.95}M_{0.05}/Al_1$ ($M = Ca, Sr$ and Ba) MMO.

Precursor Compound	Temperature	BET Surface Area m^2/g
Mg_2Al_1 precursor gels	800 °C	87.470
Mg_2Al_1	800 °C	65.450
Mg_2Al_1 precursor gels	950 °C	27.749
Mg_2Al_1	950 °C	40.528
$Mg_{1.95}Ca_{0.05}/Al_1$ precursor gels	800 °C	46.461
$Mg_{1.95}Ca_{0.05}/Al_1$	800 °C	129.16
$Mg_{1.95}Ca_{0.05}/Al_1$ precursor gels	950 °C	34.791
$Mg_{1.95}Ca_{0.05}/Al_1$	950 °C	46.078
$Mg_{1.95}Sr_{0.05}/Al_1$ precursor gels	800 °C	53.847
$Mg_{1.95}Sr_{0.05}/Al_1$	800 °C	104.543
$Mg_{1.95}Sr_{0.05}/Al_1$ precursor gels	950 °C	36.292
$Mg_{1.95}Sr_{0.05}/Al_1$	950 °C	51.961
$Mg_{1.95}Ba_{0.05}/Al_1$ precursor gels	800 °C	63.217
$Mg_{1.95}Ba_{0.05}/Al_1$	800 °C	122.486
$Mg_{1.95}Ba_{0.05}/Al_1$ precursor gels	950 °C	32.498
$Mg_{1.95}Ba_{0.05}/Al_1$	950 °C	40.576

**Figure 14.** The pore size distribution of mixed metal oxides (MMO) obtained by heating the Mg_2/Al_1 precursor gels (**top**) and obtained by heating the Mg_2/Al_1 LDHs (**bottom**) at 800 °C and 950 °C.

Surprisingly, the PSD width does not depend neither on the synthetic procedure nor on the annealing temperature. The determined average pore diameter in the mesopore region is approximately 3.0–5.5 nm. The PSD results obtained for the mixed metal oxides containing Ca, Sr, and Ba are shown in Figure 15.

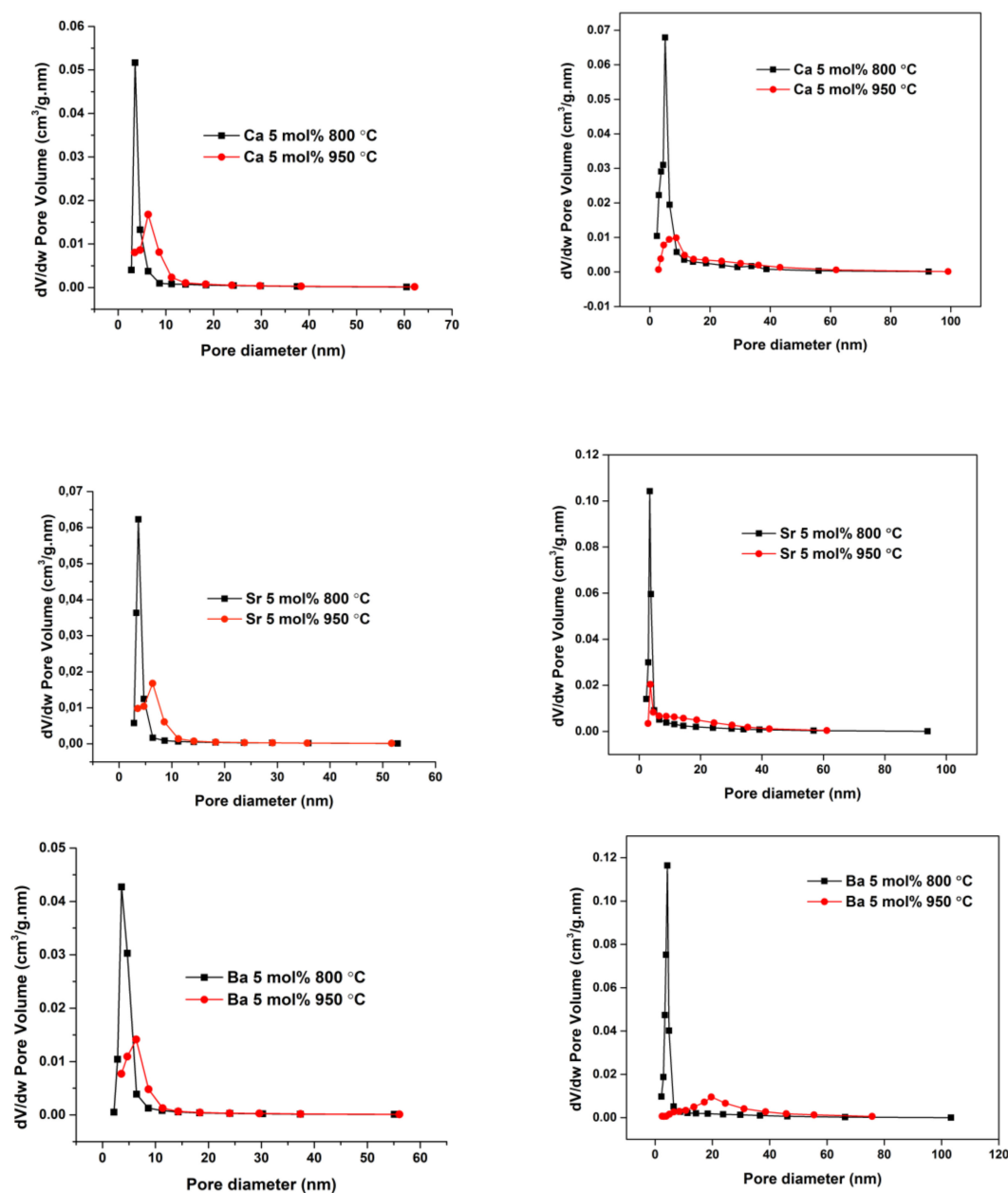


Figure 15. The pore size distribution of mixed metal oxides (MMO) obtained by heating the $\text{Mg}_{1.95}\text{Ca}_{0.05}/\text{Al}_1$ precursor gels (**top, left**), by heating the $\text{Mg}_{1.95}\text{Ca}_{0.05}/\text{Al}_1$ LDHs (**top, right**), by heating the $\text{Mg}_{1.95}\text{Sr}_{0.05}/\text{Al}_1$ precursor gels (**middle, left**), by heating the $\text{Mg}_{1.95}\text{Sr}_{0.05}/\text{Al}_1$ LDHs (**middle, right**), by heating the $\text{Mg}_{1.95}\text{Ba}_{0.05}/\text{Al}_1$ precursor gels (**bottom, left**), and by heating the $\text{Mg}_{1.95}\text{Ba}_{0.05}/\text{Al}_1$ LDHs (**bottom, right**) at 800 °C and 950 °C.

As seen, various surface properties could be detected for the MMO samples synthesized by two different methods. The pore size distribution of directly obtained MMO by heating Mg–Al–O precursor gels depends on the heating temperature and less on the nature of alkaline earth metal. The determined average pore diameter in the mesopore region is approximately 2.5–8 nm, 2.5–7 nm, and 2.5–9 nm

for the Ca-MMO, Sr-MMO, and Ba-MMO samples, respectively, synthesized at 800 °C. The pore size distribution is visible wider for the MMO synthesized at 950 °C (approximately 3–10.15 nm, 3–12.5 nm, and 3.5–10.1 nm for the Ca-MMO, Sr-MMO, and Ba-MMO samples, respectively). As seen from Figure 15, the pore size distributions obtained by the BJH method for the MMO specimens synthesized from the reconstructed Mg_2/Al_1 LDHs depends on both synthesis temperature and nature of substituent. The most narrow pore size distribution was determined for Sr-containing MMO (2.5–3.5 nm for the sample heat-treated at 800 °C). On the other hand, the sample with 5% mol of Ba and prepared at 950 °C has very broad pore size distribution. In general, the gain in the volume of mesopores is clearly visible for the MMO samples synthesized at lower temperature. However, the pore diameter, wall thickness, and pore size distribution depend on the used synthesis method, heating temperature, and nature of alkali earth metal in the MMO host matrix, indicating that these MMO could have the potential for the application as catalysts, catalyst supports, and adsorbents.

4. Conclusions

In this study, the reconstruction peculiarities of sol–gel derived $Mg_{2-x}M_x/Al_1$ ($M = Ca, Sr, Ba$) layered double hydroxides (LDHs) were investigated. For the synthesis of $Mg_{2-x}M_x/Al_1$ ($M = Ca, Sr, Ba$) LDHs, the indirect sol–gel synthesis method has been used. Citric acid and 1,2-ethanediol were used as complexing agents in sol–gel processing [39]. The mixed metal oxides (MMO) were synthesized by two different routes in this work. Firstly, the MMO were obtained directly by heating $Mg(M)-Al-O$ precursor gels at 650 °C, 800 °C, and 950 °C. The XRD pattern of the MMO sample obtained by heating $Mg-Al-O$ precursor gels at 650 °C showed the formation of monophasic MMO. However, with increasing annealing temperature up to 800 °C or 950 °C and upon the substitution of Mg by Ca, Sr, and Ba, highly crystalline spinel ($MgAl_2O_4$, $CaAl_2O_4$, $SrAl_2O_4$ and $BaAl_2O_4$) phases have also formed. All MMO samples were successfully reconstructed to the $Mg_{2-x}M_x/Al_1$ ($M = Ca, Sr, Ba$) layered double hydroxides (LDHs) in water at 50 °C for 6 h (pH 10). However, the spinel phases were not reconstructed and remained as impurity phases. Moreover, during the reconstruction process, a negligible amount of metal carbonates ($CaCO_3$, $SrCO_3$, and $BaCO_3$) have formed as well. Secondly, the MMO were also obtained by heating the reconstructed LDHs at the same temperatures and the phase composition, morphology, and surface properties of MMO were compared with obtained ones after initial annealing. It was demonstrated that the second time obtained Ca and Sr-substituted MMO samples contained more side phases. However, this was not the case for the Ba-substituted MMO samples, since both synthesis products obtained from precursor gels and by heating LDHs were composed of several crystalline phases. It was demonstrated for the first time that the microstructure of reconstructed MMO from sol–gel derived LDHs showed a “memory effect”, i.e., the microstructural features of MMO were almost identical as was determined for LDHs. Besides, the microstructure of investigated samples was not dependent on the annealing temperature and substitution. The synthesized $Mg(M)-Al$ MMO samples exhibited type IV isotherms independent of the annealing temperature. At higher pressure values, the H1 hystereses were detected, which are characteristic for the mesoporous (pore size in the range of 2–50 nm) materials. It was found that the pore size distributions obtained by the BJH method for the MMO specimens synthesized from the reconstructed Mg_2/Al_1 LDHs depended on both the synthesis temperature and nature of the substituent. The most narrow pore size distribution was determined for Sr-containing MMO (2.5–3.5 nm for the sample heat-treated at 800 °C). On the other hand, the sample with 5% mol of Ba and prepared at 950 °C had very broad pore size distribution. The pore diameter, wall thickness, and pore size distribution was found to be dependent on used synthesis method, heating temperature, and nature of alkali earth metal in the MMO host matrix.

Author Contributions: Formal Analysis, L.V., A.Z., A.I., and A.K.; Investigation, L.V., M.R., I.G.-P., A.Z., and V.P.; Resources, A.Z., A.I., and A.K.; Data Curation, L.V.; Writing—Original Draft Preparation, L.V., I.G.-P., and A.K.; Writing—Review and Editing, A.K.; Visualization, A.Z. and V.P.; Supervision, A.I. and A.K. All authors have read and agreed to the published version of the manuscript.

Funding: This work was supported by a Research grant N°CAMAT (No. S-LB-19-2) from the Research Council of Lithuania and Belarusian Republican Found for Fundamental Research (No. 19LITG-007).

Conflicts of Interest: The authors declare that they have no conflict of interest.

References

1. Li, F.; Duan, X. Applications of layered double hydroxides. In *Layered Double Hydroxides (Structure and Bonding)*; Mingos, D.M.P., Ed.; Springer-Verlag: Berlin/Heidelberg, Germany, 2006; pp. 193–223.
2. Sokol, D.; Klemkaite-Ramanauskė, K.; Khinsky, A.; Baltakys, K.; Beganskiene, A.; Baltusnikas, A.; Pinkas, J.; Kareiva, A. Reconstruction effects on surface properties of Co/Mg/Al layered double hydroxide. *Mater. Sci. (Medžiagotyra)* **2017**, *23*, 144–149. [[CrossRef](#)]
3. Mishra, G.; Dash, B.; Pandey, S. Layered double hydroxides: A brief review from fundamentals to application as evolving biomaterials. *Appl. Clay Sci.* **2018**, *1539*, 172–186. [[CrossRef](#)]
4. Vieira, D.E.L.; Sokol, D.; Smalenskaite, A.; Kareiva, A.; Ferreira, M.G.S.; Vieira, J.M.; Brett, C.M.A.; Salak, A.N. Cast iron corrosion protection with chemically modified Mg-Al layered double hydroxides synthesized using a novel approach. *Surf. Coat. Technol.* **2019**, *375*, 158–163. [[CrossRef](#)]
5. Smalenskaite, A.; Pavasaryte, L.; Yang, T.C.K.; Kareiva, A. Undoped and Eu³⁺ doped magnesium-aluminium layered double hydroxides: Peculiarities of intercalation of organic anions and investigation of luminescence properties. *Materials* **2019**, *12*, 736. [[CrossRef](#)] [[PubMed](#)]
6. Li, Y.L.; Ma, J.; Yuan, Y.X. Enhanced adsorption of chromium by stabilized Ca/Al-Fe layered double hydroxide decorated with ferric nanoparticles. *Sci. Adv. Mater.* **2020**, *12*, 441–448. [[CrossRef](#)]
7. Zhang, Z.D.; Qin, J.Y.; Zhang, W.C.; Pan, Y.T.; Wang, D.Y.; Yang, R.J. Synthesis of a novel dual layered double hydroxide hybrid nanomaterial and its application in epoxy nanocomposites. *Chem. Eng. J.* **2020**, *381*, 122777. [[CrossRef](#)]
8. Sato, T.; Fujita, H.; Endo, T.; Shimada, M.; Tsunashima, A. Synthesis of hydrotalcite-like compounds and their physico-chemical properties. *Reactiv. Solids* **1988**, *5*, 219–228. [[CrossRef](#)]
9. Klemkaite, K.; Prosycevas, I.; Taraskevicius, R.; Khinsky, A.; Kareiva, A. Synthesis and characterization of layered double hydroxides with different cations (Mg, Co, Ni, Al), decomposition and reformation of mixed metal oxides to layered structures. *Centr. Eur. J. Chem.* **2011**, *9*, 275–282. [[CrossRef](#)]
10. Salak, A.N.; Tedim, J.; Kuznetsova, A.I.; Ribeiro, J.L.; Vieira, L.G.; Zheludkevich, M.L.; Ferreira, M.G.S. Comparative X-ray diffraction and infrared spectroscopy study of Zn-Al layered double hydroxides: Vanadate vs. nitrate. *Chem. Phys.* **2012**, *397*, 102–108. [[CrossRef](#)]
11. Meyn, M.; Beneke, K.; Lagaly, G. Anion exchange reactions of layered double hydroxides. *Inorg. Chem.* **1990**, *29*, 5201–5206. [[CrossRef](#)]
12. Newman, S.P.; Jones, W. Synthesis, characterization and applications of layered double hydroxides containing organic guests. *New J. Chem.* **1998**, *22*, 105–115. [[CrossRef](#)]
13. Olf, H.W.; Torres-Dorante, L.O.; Eckelt, R.; Kosslick, H. Comparison of different synthesis routes for Mg-Al layered double hydroxides (LDH): Characterization of the structural phases and anion exchange properties. *Appl. Clay Sci.* **2009**, *43*, 459–464. [[CrossRef](#)]
14. Smalenskaite, A.; Vieira, D.E.L.; Salak, A.N.; Ferreira, M.G.S.; Katelnikovas, A.; Kareiva, A. A comparative study of co-precipitation and sol-gel synthetic approaches to fabricate cerium-substituted Mg/Al layered double hydroxides with luminescence properties. *Appl. Clay Sci.* **2017**, *143*, 175–183. [[CrossRef](#)]
15. Sokol, D.; Salak, A.N.; Ferreira, M.G.S.; Beganskiene, A.; Kareiva, A. Bi-substituted Mg₃Al-CO₃ layered double hydroxides. *J. Sol-Gel Sci. Technol.* **2018**, *85*, 221–230. [[CrossRef](#)]
16. Smalenskaite, A.; Salak, A.N.; Kareiva, A. Induced neodymium luminescence in sol-gel derived layered double hydroxides. *Mendeleev Commun.* **2018**, *28*, 493–494. [[CrossRef](#)]
17. Smalenskaite, A.; Kaba, M.M.; Grigoraviciute-Puroniene, I.; Mikoliunaite, L.; Zarkov, A.; Ramanauskas, R.; Morkan, I.A.; Kareiva, A. Sol-gel synthesis and characterization of coatings of Mg-Al layered double hydroxides (LDHs). *Materials* **2019**, *12*, 3738. [[CrossRef](#)]
18. Valeikiene, L.; Paitian, R.; Grigoraviciute-Puroniene, I.; Ishikawa, K.; Kareiva, A. Transition metal substitution effects in sol-gel derived Mg_{3-x}M_x/Al₁ (M = Mn, Co, Ni, Cu, Zn) layered double hydroxides. *Mater. Chem. Phys.* **2019**, *237*, 121863. [[CrossRef](#)]

19. Kovanda, F.; Grygar, T.; Dornicak, V. Thermal behaviour of Ni-Mn layered double hydroxide and characterization of formed oxides. *Solid State Sci.* **2003**, *5*, 1019–1026. [[CrossRef](#)]
20. Liu, X.W.; Wu, Y.L.; Xu, Y.; Ge, F. Preparation of Mg/Al bimetallic oxides as sorbents: Microwave calcination, characterization, and adsorption of Cr(VI). *J. Solid State Chem.* **2016**, *79*, 122–132. [[CrossRef](#)]
21. Vicente, P.; Perez-Bernal, M.E.; Ruano-Casero, R.J.; Ananias, D.; Almeida Paz, F.A.; Rocha, J.; Rives, V. Luminescence properties of lanthanide-containing layered double hydroxides. *Microp. Mesop. Mater.* **2016**, *226*, 209–220. [[CrossRef](#)]
22. Kryshab, T.; Calderon, H.A.; Kryvko, A. Microstructure characterization of metal mixed oxides. *MRS Adv.* **2017**, *2*, 4025–4030. [[CrossRef](#)]
23. Bugris, V.; Adok-Sipiczki, M.; Anitics, T.; Kuzmann, E.; Homonnay, Z.; Kukovecz, A.; Konya, Z.; Sipos, P.; Palinko, I. Thermal decomposition and reconstruction of CaFe-layered double hydroxide studied by X-ray diffractometry and Fe-57 Mossbauer spectroscopy. *J. Molec. Struct.* **2015**, *1090*, 19–24. [[CrossRef](#)]
24. Millange, F.; Walton, R.L.; O'Hare, D. Time-resolved in situ X-ray diffraction study of the liquid-phase reconstruction of Mg-Al-carbonate hydrotalcite-like compounds. *J. Mater. Chem.* **2000**, *10*, 1713–1720. [[CrossRef](#)]
25. Li, L.; Qi, G.X.; Fukushima, M.; Wang, B.; Xu, H.; Wang, Y. Insight into the preparation of Fe₃O₄ nanoparticle pillared layered double hydroxides composite via thermal decomposition and reconstruction. *Appl. Clay Sci.* **2017**, *140*, 88–95. [[CrossRef](#)]
26. Bernardo, M.P.; Ribeiro, C. Zn-Al-based layered double hydroxides (LDH) active structures for dental restorative materials. *J. Mater. Res. Technol.* **2019**, *8*, 1250–1257. [[CrossRef](#)]
27. Elhalil, A.; Elmoubarki, R.; Machrouhi, A.; Sadiq, M.; Abdennouri, M.; Qourzal, S.; Barka, N. Photocatalytic degradation of caffeine by ZnO-ZnAl₂O₄ nanoparticles derived from LDH structure. *J. Environ. Chem. Eng.* **2017**, *5*, 3719–3726. [[CrossRef](#)]
28. Valente, J.S.; Lima, E.; Toledo-Antonio, J.A.; Cortes-Jacome, M.A.; Lartundo-Rojas, L.; Montiel, R.; Prince, J. Comprehending the thermal decomposition and reconstruction process of sol-gel MgAl layered double hydroxides. *J. Phys. Chem. C* **2010**, *114*, 2089–2099. [[CrossRef](#)]
29. Venugopal, B.R.; Shivakumara, C.; Rajamathi, M. A composite of layered double hydroxides obtained through random costacking of layers from Mg-Al and Co-Al LDHs by delamination-restacking: Thermal decomposition and reconstruction behavior. *Solid State Sci.* **2007**, *9*, 287–294. [[CrossRef](#)]
30. Chagas, L.H.; de Carvalho, G.S.G.; Carmo, W.R.D.; Gil, R.A.S.S.; Chiaro, S.S.X.; Leitao, A.A.; Diniz, R.; de Sena, L.A.; Achete, C.A. MgCoAl and NiCoAl LDHs synthesized by the hydrothermal urea hydrolysis method: Structural characterization and thermal decomposition. *Mater. Res. Bull.* **2015**, *64*, 207–215. [[CrossRef](#)]
31. Kim, B.K.; Gwak, G.H.; Okada, T.; Oh, J.M. Effect of particle size and local disorder on specific surface area of layered double hydroxides upon calcination-reconstruction. *J. Solid State Chem.* **2018**, *263*, 60–64. [[CrossRef](#)]
32. Seftel, E.M.; Ciocarlan, R.G.; Michielsen, B.; Meynen, V.; Mullens, S.; Cool, P. Insights into phosphate adsorption behavior on structurally modified ZnAl layered double hydroxides. *Appl. Clay Sci.* **2018**, *165*, 234–246. [[CrossRef](#)]
33. Lee, S.H.; Tanaka, M.; Takahashi, Y.; Kim, K.W. Enhanced adsorption of arsenate and antimonate by calcined Mg/Al layered double hydroxide: Investigation of comparative adsorption Check for mechanism by surface characterization. *Chemosphere* **2018**, *211*, 903–911. [[CrossRef](#)] [[PubMed](#)]
34. Kang, J.; Levitskaia, T.G.; Park, S.; Kim, J.; Varga, T.; Um, W. Nanostructured MgFe and CoCr layered double hydroxides for removal and sequestration of iodine anions. *Chem. Eng. J.* **2020**, *380*, 122408. [[CrossRef](#)]
35. Santos, R.M.M.; Tronto, J.; Briois, V.; Santilli, C.V. Thermal decomposition and recovery properties of ZnAl-CO₃ layered double hydroxide for anionic dye adsorption: Insight into the aggregative nucleation and growth mechanism of the LDH memory effect. *J. Mater. Chem. A* **2017**, *5*, 9998–10009. [[CrossRef](#)]
36. Cao, Y.; Wang, Y.X.; Zhang, X.Y.; Cai, X.G.; Li, Z.H.; Li, G.T. Facile synthesis of 3D Mg-Al layered double oxide microspheres with ultra high adsorption capacity towards methyl orange. *Mater. Lett.* **2019**, *257*, 126695. [[CrossRef](#)]
37. Belskaya, O.B.; Leont'eva, N.N.; Gulyaeva, T.I.; Cherepanova, S.V.; Talzi, V.P.; Drozdov, V.A.; Likholobov, V.A. Influence of a doubly charged cation nature on the formation and properties of mixed oxides MAlO_x (M = Mg²⁺, Zn²⁺, Ni²⁺) obtained from the layered hydroxide precursors. *Russ. Chem. Bull.* **2013**, *62*, 2349–2361. [[CrossRef](#)]

38. Zhao, Y.; Li, J.-G.; Fang, F.; Chu, N.; Ma, H.; Yang, X. Structure and luminescence behaviour of as-synthesized, calcined, and restored MgAlEu-LDH with high crystallinity. *Dalton Trans.* **2012**, *41*, 12175–12184. [[CrossRef](#)]
39. Ishikawa, K.; Garskaite, E.; Kareiva, A. Sol-gel synthesis of calcium phosphate-based biomaterials -A review of environmentally benign, simple and effective synthesis routes. *J. Sol-Gel Sci. Technol.* **2020**, *94*, 551–572. [[CrossRef](#)]



© 2020 by the authors. Licensee MDPI, Basel, Switzerland. This article is an open access article distributed under the terms and conditions of the Creative Commons Attribution (CC BY) license (<http://creativecommons.org/licenses/by/4.0/>).